FAULT TOLERANT FLIGHT CONTROLLER FOR A HIGH PERFORMANCE FIGHTER AIRCRAFT DURING AUTO-LANDING

Mr. NAGARAJ RAMRAO
Director, Centre for Cognitive Technologies,
Department of Electronics & Communication Engineering,
R. V. College of Engineering, Bangalore, INDIA
Mr. NIKHIL SANTOSH & ROHIT PANIKKAR, UG Students
Dr. T.V. RAMAMURTHY,
Professor & HOD, Department of Electronics & Communication Engineering,
Sir M. Visvesvaraya Institute of Technology, Bangalore, INDIA
Visvesvaraya Technological University, Karnataka, INDIA
http://www.rvce.ac.in

Abstract:- In this paper the auto-landing problem of a high performance fighter aircraft has been addressed. During landing, the flight path consists of flight segments such as a wing-level flight, a coordinated turn, glide slope descent and finally the flare maneuver and touchdown on the runway. The trajectory segments corresponding to these phases have to be flown in the presence of severe winds. A detailed description of the wind model is also being considered. These tend to cause deviation of the aircraft from the specified trajectory. However, it has to be ensured that all trajectory deviations are within specified limits. The touch conditions are given with tight specifications, named for convenience as the *touch-down pill box*. The controller is first designed to meet all these specifications for all these phases under no failure conditions of the actuators. We then augment the controller to be able to handle the same flight segments but with the occurrence of certain failure conditions of the actuators.

Keywords:- Auto Landing, Ailerons, Elevators, Basic trajectory following controller, pill box specifications

1 Introduction

The path followed by the aircraft starts off with stable, level flight and ends with the aircraft safely landing on the ground, within the boundaries of the runway. We analyze the problem, by dividing the entire flight path into seven distinct segments as shown in **Figure 1**.

1.1 Criteria for Controller design

The design of the controller should be such that several safety and performance criteria are met in order to ensure a safe and successful landing. These include bounds on the flight parameters such as lateral deviation, altitude, heading angle, flight path angle and airspeed. We therefore define the *touch-down pillbox* region as depicted in **Table 1**, i.e. the boundary within which the aircraft must land under the specified conditions. The controller is designed to operate even during the occurrence of failure and is said to have successfully taken care of failures in a given region only if the aircraft lands within the pillbox.

The minimum velocity specification is to ensure that the aircraft does not go into a stall during its final approach. The flight path angle limit is required so that the angle of descent is not too steep and a limit on the bank angle ensures that the wings do not collide with the ground.

Under moderate turbulence conditions, the mean actuator rates for aileron, elevator, and rudder should be less than 33% of the maximum rates, and the mean throttle rate should be less than 15% of the maximum rate. The maximum deflection rates for the aerodynamic control surfaces are 60deg/sec.

1.2 Wind Profiles

There are two wind components which we consider during landing as shown in **Figure 2.** One is a microburst that is in the vertical direction and the other is the lateral wind (in a direction perpendicular to the runway).

2 The Basic Trajectory Following Controller (BTFC)

Figure 3 illustrates the various blocks used in the design of the control scheme. The basic aim of designing the control scheme for following the specified trajectory consists of two parts – a tracking command generator and the classical feedback controller. The tracking command generator is a part of the feedback loop and generates the command signals based on trajectory deviations. These command signals are then used by the controller as its inputs. For the purpose of our simulations and analysis a reasonable worst case delay of 40msec due to sampling, which is twice the controller sampling interval, was added in the loop. This is shown by the sampling delay block in the **Figure 3**.

The desired trajectory may either be a straight line path or a curved path. It is with the help of the tracking command generator that the offset of the aircraft from this desired path can be found for each segment of the flight. As can be seen from the block diagram above, the tracking command generator computes a reference command '**r**' specifying the Altitude, Velocity and the Cross Distance from the desired track. It also generates the angular error of the aircraft velocity vector from the desired track vector. In case of the straight line segments, the cross distance is simply the length of the perpendicular, whereas in case of circular arcs, this distance is the difference between the distance to the centre of the circular arc and the radius of the turn. We also need to calculate the angular error of the velocity vector.

The Classical Feedback Controller uses these desired values of altitude, velocity and the track angle as references and also simultaneously tries to make the error minimum which is in this case the deviation from the desired trajectory.

3 Failure Scenarios

In this paper we have considered five types of failures including a single control surface failure as well as the failure of a combination of control surfaces, as tabulated in **Table 2**. We have ignored the case of the failure scenario where both the elevators fail because this case is in general, not recoverable. The simulation results for all the 4 cases have been obtained.

Under normal flight conditions the two elevators are always commanded together. But when they are used differentially they can be used to produce roll moment as well. Examination of the input matrix shows that in the differential mode, the elevators are about 60% as effective as the ailerons in producing roll moment. As a result the elevators can be used to produce pitching and roll moment. This is as opposed to the ailerons that are not effective in producing any pitching moment. Hence we can consider the case where both the ailerons fail and by using elevators in differential mode we can get the aircraft back to equilibrium.

When the control surface(s) fail, their resultant hard over position could be one from among any value within the permissible range of deflections. Clearly, all possible hard over positions are not feasible, because in some cases the resulting moments cannot be trimmed out for the landing maneuver (i.e., a steady level turn or wing level descent). Thus, the full range of hard over positions must be checked for the feasible subset. The feasible range must be computed by trimming the aircraft model with surfaces in failed position. If trim is achieved then that particular failed position belongs to the feasible region. The feasible region is the union of the following trim computations:

- Region of level flight trim ($p = q = r = \gamma = 0$, 6-DOF accelerations = 0)
- Region of level descent trim ($p = q = r = 0$, $\gamma = -6$deg, 6-DOF accelerations = 0)
- Region of level turning trim ($\varphi = 40$ deg, 6-DOF accelerations = 0)

Figure 4 shows the trim computations for the three trim conditions for left elevator failure. It is seen that the level turn set lies in the intersection of all the three conditions, as it is the most demanding maneuver. Therefore, it determines the feasible region. **Figures 5** through **8** show the results for left aileron and combination failures. Similar conclusions are valid for these failures.

3.1 Failure Injection Point

The landing trajectory used for the simulations is discussed earlier. The point in time at which elevator or aileron control surface failures are introduced will have some impact on the final outcome and failure tolerance. These failure points are not known in advance and could occur at random. It is postulated in this report that since the level turn is the deciding factor for the feasible region computations, the failures will have maximum impact when they occur before the turn is initiated. The controller will then have to ensure that the aircraft safely negotiates the turn along with the descent phase of the landing trajectory. Thus, in all the simulation results presented in this report, the failures occur at 10 seconds for the elevator and 8 seconds for either aileron, both of which occur before the turn initiation.

4 BTFC Design

BTFC is as shown in **Fig.3**. The trajectory following control design task is divided into two parts - a reference command generator whose outputs are acted upon by the classical feedback controller. In the design of the controller a worst-case delay of 40msec (twice the controller sample rate) was introduced in the loop in all the simulations and analysis.

4.1 Design & Operation

The BTFC is designed using the classical loop shaping SISO design techniques. It is assumed that the angle of attack and sideslip is not available for feedback. The reference command generator or tracking controller as it is called in **Figure 3**, determines the offset of the aircraft from the desired ground track for each segment of the flight and computes the reference commands (labeled '**r**' in Figure 3) consisting of Altitude, Velocity and Cross Distance from the desired track and the angular error of the aircraft velocity from the desired track vector. The segments of trajectory are either straight lines or arcs of circles. Thus, the cross distance is simply the length of the perpendicular in case of the line segments. In case of the circular arc, this quantity is the difference between the distance to the center of the circular arc and the radius of the turn. Similarly, the angular error can be calculated using the components of the aircraft velocity in the X-Y plane and the direction of the desired trajectory nearest to the aircraft. Once these quantities are known, the velocity and altitude references are obtained by linear interpolation between the end point values at the ends of each segment.

4.2 Longitudinal Axis Design

Figure 9 depicts the overall control scenario in longitudinal axis design. The innermost loop in the longitudinal axis is the pitch rate loop designed for recovering the stability. The velocity to throttle loop is designed next. A five second lag is assumed to be present in this loop. This is to represent the lag in response from the engine due to throttle movement. A lead-lag compensator with a gain of $\mathbf{0.032}\ m^{-1}s$ is placed in the forward path of this loop.The final structure of the longitudinal controller is in the form of a cascade. The inner most loop is the pitch rate loop. It is also the fastest loop and therefore must be used to address the robustness aspect of the design with respect to control surface failures.

The "from roll axis" is used for the two aileron failure case where in it is used to induce differential elevator behavior. When a Type V failure, that is both the left and right ailerons fail, occurs, the standard BTFC based controller is unable to handle this situation. Failure of both ailerons implies that there is no control surface present to induce roll of the aircraft. We overcome the above situation by making use of the fact that the elevators of the aircraft when used in differential mode can be used to introduce roll and are 60% as effective as the ailerons in inducing roll.

In order to incorporate this property into the controller design we induce differential control for the elevators, where in each elevator receives a signal proportional to the error signal caused by failure of the aileron. The error caused by aileron failure is added to one of the elevators and subtracted from the other thereby causing their differential motion. The elevators thus operate in combined mode so as to produce the pitching moment and in differential mode to induce rolling, thereby compensating for the loss of both ailerons.

The longitudinal model designed and analyzed is explained in what follows. It is observed that the contributing elements are those of the airspeeds in the X and Z planes(u, w), the pitch rate (p) and the pitch angle (θ). The 4x4 matrix of the longitudinal model is created using these elements. The input deflection angles that influence the output pitch rate q, are those of the combined elevator, δec, and the differential elevator, δed. The combined elevator parameter is achieved by adding the left and right elevator deflections, ie., $\delta er + \delta el$. The differential elevator is obtained by subtracting the same elements for this longitudinal axis design. The lateral directional model is discussed under the following heading.

4.3 Lateral-Directional Axis Design

The innermost loop in the lateral axis is the roll rate loop designed for achieving crisp roll rate response. The yaw rate feedback in the inner most loop in the directional axis is designed to improve the damping of the Dutch Roll mode and suppress sideslip development.

Examination of the equations of motion, indicate that the sideslip rate can be approximated by two components. The first is the term $r - p \tan \alpha$ and the other is the lateral acceleration. Since, it is our intention to minimize the sideslip, a combination of these two quantities is used. A PID design was attempted on the track angle deviation. The integral of track angle deviation is simply the track deviation in meters. The derivative part was replaced with a feed forward correction using the reference track angle deviation. Aileron to rudder interconnect gain of 1.2deg/deg is introduced to provide an open loop sideslip reduction. The final scheme is as shown in **Figure 10**. The response of this closed loop system is shown in the **Figure 11.** It is seen that for a heading change from 0 to 90 degrees, the closed loop deviation in track error is less than ±100meters, the sideslip deviation is less than ±2degrees and the bank angle required is less than 60degrees.

The lateral directional model, similar to the longitudinal model is designed as follows. Here the contributing elements, are those of the airspeed in the Y-axis, v, the roll and yaw rates in the X and Z axes, (p,r), and the yaw angle, ψ. The deflections that affect the roll and yaw rates are those of the aileron (δa) and rudder (δr). The deflections of the left and right aileron are summed to obtain this scheme. (ie., $\delta a = \delta al+\delta ar$).

5 Robustness of Design

The above design was checked for robustness and can handle C.G. variation from 32% MAC (Mean Aerodynamic Chord) to 37% MAC. The C.G variation in the horizontal direction has negligible effect on the lateral-directional closed loop system. The step and ramp responses of the altitude closed loop under a change of ±20% change of mass show that responses are not significantly different either for the longitudinal or the lateral directional axes.

6 Simulation Results

Simulation of landing trajectory is shown in **Fig.11**, in the presence of winds and no failures. In all the figures for sideslip, altitude and velocity, numbers at the top line of the plots marks the segments of the trajectory. For example, 1 represents first straight line segment of level flight, followed by 2 showing the right turn. 3 represents level flight after the turn and so on. The simulation was stopped as soon as the landing gear touched the ground. In the velocity, X-Y and altitude plots, the reference signal and the aircraft response both are trajectory and touch down point as per the *pill-box* specifications. There is an initial jump the velocity at t=0, because the model was trimmed for straight level flight and the gust shown in was introduced at t = 0 resulting in an instantaneous increase in forward velocity. This perturbation died out. Subsequently, the velocity shows a dip in Segment 2 due to the initial loss of lift during beginning of the turn.

Velocity deviation seen at the beginning of the 4th and 5th segments is due to change in glide slope. The velocity disturbances at about 120 and 130 sec are due to appearance of wind shear of magnitude –12m/s and 23m/s (-12m/s to 11m/s) respectively. Lateral deviation in ground track appears in the X-Y plane during the turn in the 2nd and 3rd, eventually being corrected by the 3rd segment. There is also a correspondingly small but noticeable deviation in sideslip during these phases, which is corrected rapidly. In the 4th and 5th segments the sideslip shows a large deviation from the desired (zero) value due to the side gusts of magnitude +7 m/s and -14 m/s (+7 m/s to -7 m/s) respectively.

The main purpose in designing this controller is to determine the best possible performance that can be expected from the classical architecture. The single failure of the left elevator, stuck at a hard over deflection of –14 degrees at 10 seconds results in a time response obtained during the landing task as shown in **Fig 11. Fig.12** shows the feasible region and the failure tolerance region for the single elevator failure (Type I). **Figures 13 through 15** present the failure tolerance of the CGTFC to Type II, III, IV, V failures

7 CONCLUSIONS

The BTFC is designed for landing under no failures. An important assumption in this design is that the angle of attack and sideslip are not available for feedback. This controller is robust to changes in aircraft speed, roll inertia, mass and loop delay. It also has limited tolerance to C.G. variation. The pitch rate and roll rate gains can be increased to make the controller more robust. The baseline controller (BTFC) designed using classical single axis SISO techniques (longitudinal and lateral directional design) can be modified to handle type V failure. The innermost loop gain of the classical controller is critical in determining the level of failure tolerance. The outer loop gains should be sufficient to achieve good trajectory following. However, they must not be very high as this will result in saturation of the actuators due to large wind disturbance.

FIGURES

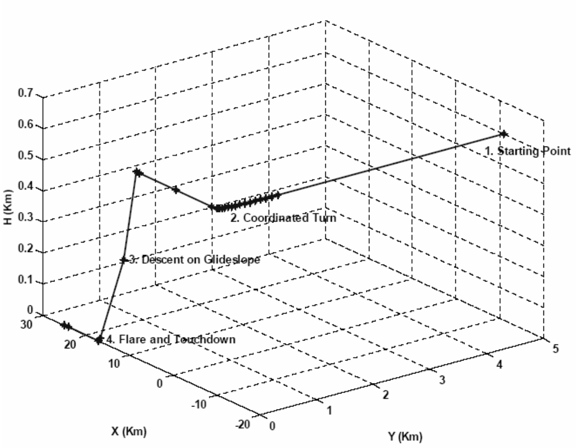

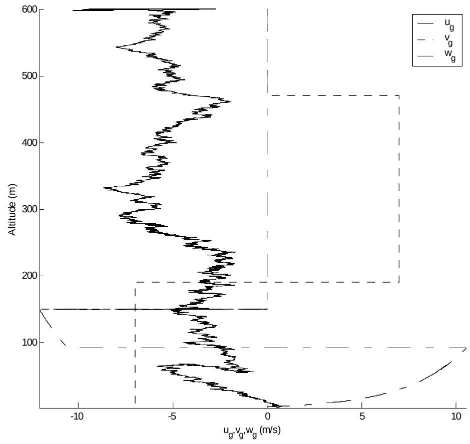

Figure 1:Flight path during touch down

Figure 2:Wind Profiles during mission

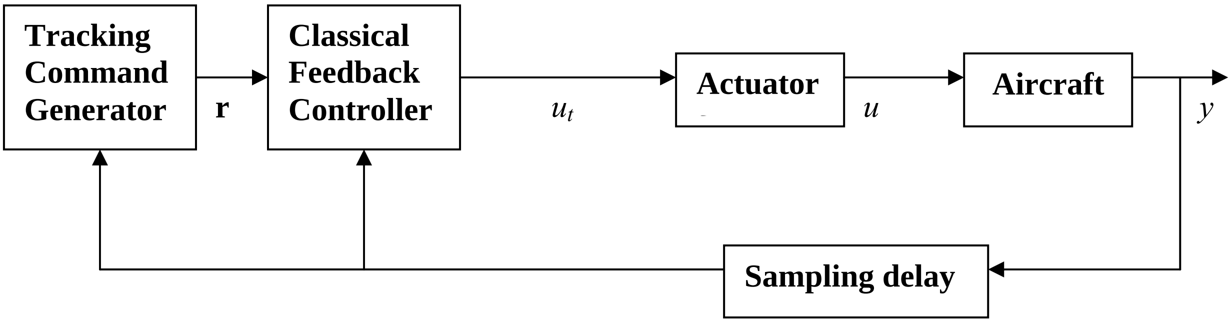

Figure 3: Design philosophy for BTFC

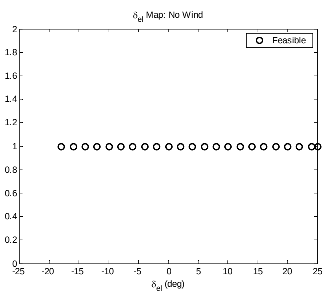

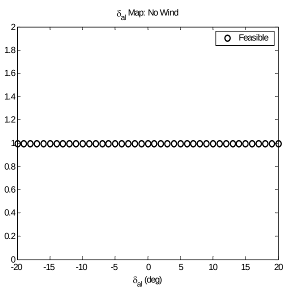

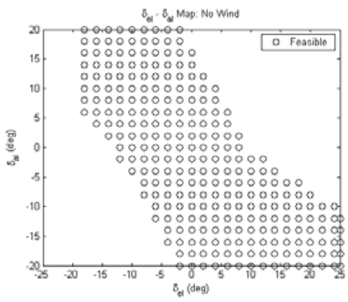

Fig 4 Feasible range for left elevator alone failure

Fig 5. Feasible range for left aileron alone failure

Fig6. Feasible range for left elevator – left aileron combination failure

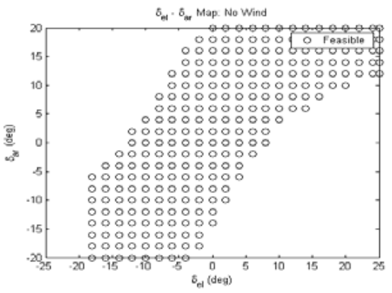

Fig 7. Feasible range for left elevator – right aileron combination failure

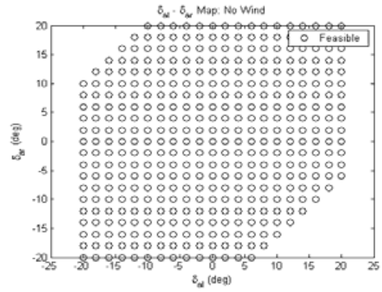

Fig 8. Feasible range for left aileron – right aileron combination failure

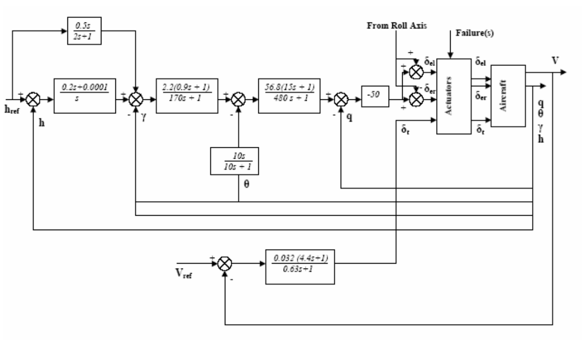

Figure 9: Longitudinal Axis Design

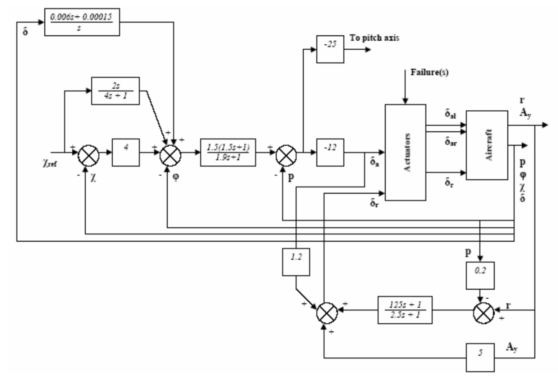

Figure 10. Lateral Axis Design

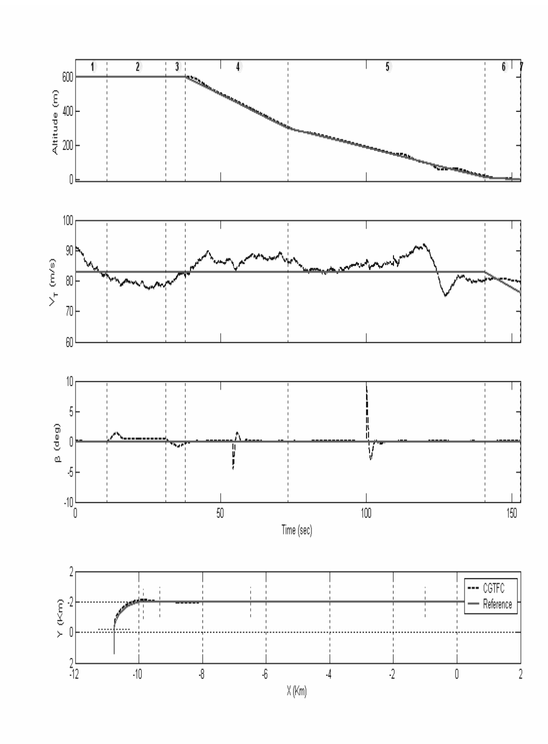

Figure 11:Response of BTFC under no failures

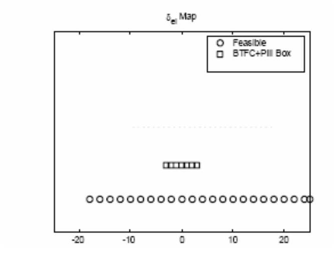

Fig. 12 – Left elevator failure tolerance of BTFC

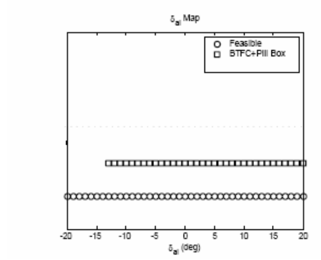

Fig. 13– Left aileron failure tolerance of BTFC

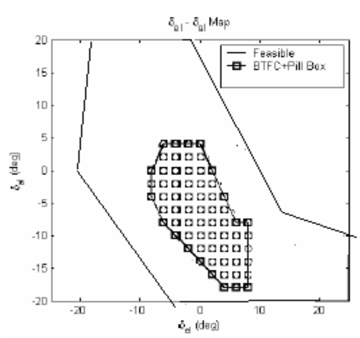

Fig.14- Left elevator and left aileron failure tolerance of the BTFC

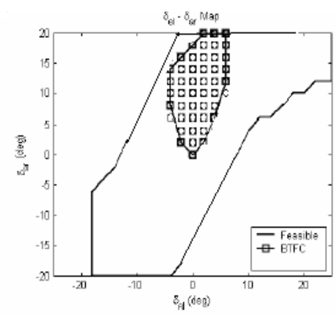

Fig. 15– Left elevator and right aileron tolerance of the BTFC

TABLES

Table 1 : Pill - Box Specifications

X-distance	-100m ≤ x ≤ 300m
Y-distance	|y| ≤ 5m
Total Velocity	$V_T \geq 60$ m/s
Flight Path	γ ≤ 0.7 degrees
Bank Angle	|Φ| ≤10 degrees

TABLE 2: Failure scenario

Failure Type	Description
Type I	Failure of any one Elevator
Type II	Failure of any one Aileron
Type III	Failure of the Left Elevator and the Left Aileron
Type IV	Failure of the LeftElevator and the Right Aileron
Type V	Failure of the Left Aileron and the Right Aileron

Table 3– Comparison of Gain and Phase margins for the old and new state models.

	Gain Margin (dB)		Phase Margin (Degrees)	
	Without Differential Elevator	With Differential Elevator	Without Differential Elevator	With Differential Elevator
p	5.1	26.1	90.4	-176
q	20.2	20.2	155	155
$r - p\tan\alpha$	0.11	4.93	174	115

References

[1]Duke, Eugene L., Robert F. Antoniewicz, et.al, “Derivation and Definition of a Linear Aircraft Model”, NASA Reference Publication 1207, August 1988.

[2]Donald McLean, *Automatic Flight Control System*, Prentice Hall, Englewoods Cliffs, New Jersey, 1990.

[3]Anderson, J.D., *Introduction to Flight*, 3rd Edition, McGraw-Hill, New York, 1989.

[4]Stevens, Brian L., Frank L. Lewis, *Aircraft Control and Simulation*, John Wiley and Sons, New York, 1992.

[5]Roskam, Jan, *Airplane Flight Dynamics and Automatic Flight Controls*, Part I, Design, Analysis and Research Corporation, Lawrence, Kansas, 1995.

[6]Simpson, P.K., *Artificial Neural Systems: Foundations, Paradigms, Applications, and Implementations*, Pergamon Press, New York, 1990.

[7]Rumelhart, D. and McClelland, J., “*Parallel Distributed Processing*”, MIT Press, Cambridge Ma., 1986.

[8]Alfonso C. Paris, “Estimation of the Longitudinal and Lateral-Directional Aerodynamic Parameters from Flight Data for the NASA F/A-18 HARV”, Ph.D Dissertation, Department of Mechanical and Aerospace Engineering, West Virginia University, 1997. 178

[9]Napolitano, M.R., Dale A. Windon II et. al., “Virtual Flight Data Recorder: A Neural Extension of Existing Capabilities” Journal of Guidance, Control, and Dynamics, Vol. 21, No. 4, pp.662~664, 1998.

[10]K. J. Hunt, D. Sbardato, R. Zbikowski, and P. J. Gawthrop, “Neural Networks for Control Systems- A Survey”, Automatica, Vol. 28, No. 6, pp.1083~1112, 1992.

[11]H. Gomi and M. Kawato, “Neuralnetwork control for a closed-loop system using feedback-error-learning”, *Neural Networks*, Vol.6, No.7, 1993, pp.933-946.

[12]Cybenko, G. “Approximation by Superposition of Sigmoidal Functions”, Mathematics of Control Signals and Systems, Vol.2, No.4, pp.303~309, 198